Compound of echo-envelope statistics by beam steering for echo-envelope analysis of ultrasound image

Chihiro Nara[‡], Kenji Yoshida, Tadashi Yamaguchi, and Shinnosuke Hirata[*] (Chiba Univ.).

1. Introduction

An ultrasound pulse irradiated from the body surface is reflected (scattered) at the boundaries of the characteristic acoustic impedances within the body. The ultrasound image is formed by the scattered pulses (echoes) arranged spatiotemporally. The boundary can be regarded as the scatterer. In case there are multiple scatterers within the region corresponding to the point spread function (PSF) of the echo, the texture (echo-envelope distribution) of the ultrasound image represents the speckle pattern (the result of interference of multiple echoes) and does not directly correspond to the distribution of scatterers.

Statistical analysis of the echo envelope of ultrasound images can be used to estimate scatterer's information, such as the number density and the homogeneity of the distribution. However, the influence of statistical fluctuations is an issue in the application to diagnostic imaging. If the analysis area is expanded to reduce fluctuations, the spatial resolution of the analysis is reduced. [1]

In this study, multiple different ultrasound images of the same region were formed by steering the ultrasound beam. Then, the echo-envelope statistics calculated in each image were compounded. The suppression of the statistical fluctuation by the compound was verified using a tissue-mimicking phantom.

2. Method

2.1 Tissue-mimicking phantoms

Two types of tissue-mimicking phantoms with different scatterer densities were fabricated for echo-envelope statistics analysis in this study. The components of the low-density phantom were 95.8 wt% ultrapure water, 2 wt% polyamide (nylon 12) particles of 10 μm diameter (as scatterers), 2 wt% agar, and 0.2 wt% dispersant. The number density is equivalent to the mass density. The components of the high-density phantom were 92.5 wt% ultrapure water, 5 wt% polyamide particles of 10 μm diameter, 2 wt% agar, and 0.5 wt% dispersant.

Both phantoms were formed in a container with dimensions of 10.5 mm width, 2 mm thickness, and 7.5 mm height. The imaging was performed from above after removal from the container.

2.2 Ultrasound imaging

RF echo data were acquired using the research ultrasound system (Vantage 256, Verasonics) and two linear array probes (L11-5v and L39-21gD, Verasonics). The opening widths were 38.4 and 7.04 mm, and the element pitches were 0.3 and 0.055 mm. The center frequencies of ultrasound pulses transmitted from each probe were 7.8125 and 31.25 MHz, and the sampling frequencies were 62.5 and 125 MHz, respectively.

The beam steering of plane wave transmission was performed at 3° intervals over a range of ±15°. Pulse compression using the 11-bit Barker code was applied to improve the SNR of the received signal only for L39-21gD. A Delay-And-Sum beamforming was applied to the received signals to produce the ultrasound images with a pixel spacing of 10 μm for L11-5v and 5 μm for L39-21gD.

2.3 Echo-envelope statistics

The 3rd-order moment was investigated as an echo-envelope statistic in this study. Before calculating the 3rd-order moments in the ultrasound image, the effects of the beam profile and attenuation were removed by the normalization of the images. The root mean square (RMS) of echo envelopes in the elliptical regions centered on the pixel of interest were used for normalization. The sizes of elliptical regions were 1.44 mm in depth and 7.2 mm in lateral for L11-5v and 0.48 mm in depth and 2.4 mm in lateral for L39-21gD. Then, the 3rd-order moments in the same regions were calculated.

3. Results and discussion

Figure 1 shows 3rd-order-moment maps calculated from the ultrasound images of the high-density phantom by using L11-5v, and **Fig. 2** shows those by using L39-21gD. In Figs. 1 and 2, the positions of high values are different in each image of the beam steering. Then, the variances of the 3rd-order moments are decreased by the compound.

For quantitative evaluation of the effect of the compound, the box-and-whisker plots of 3rd-order moments in the regions of interest (ROIs) were created, as shown in **Figs. 3** and **4**. The triangle ROI in Fig. 2 corresponded to the region where all steering beams overlapped. The triangle ROI in Fig.

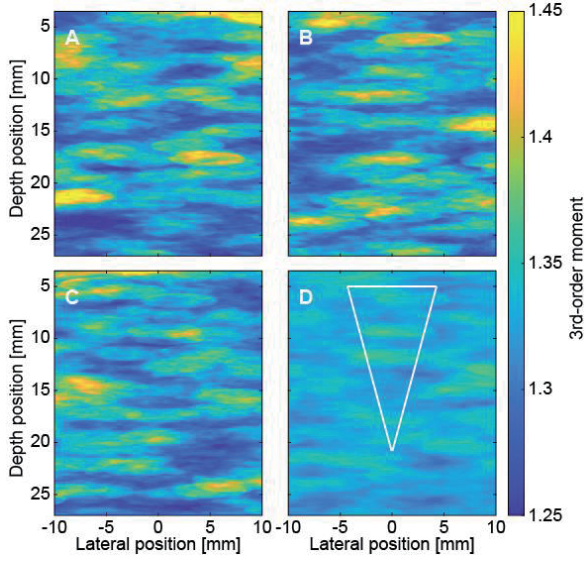E-mail: [‡]chihiro.nara@chiba-u.jp, [*]shin@chiba-u.jp

Fig. 1 3rd-order-moment maps of ultrasound images acquired using L11-5v, the steering angles of -15° (A), 0° (B), 15° (C), and the compounded one (D).

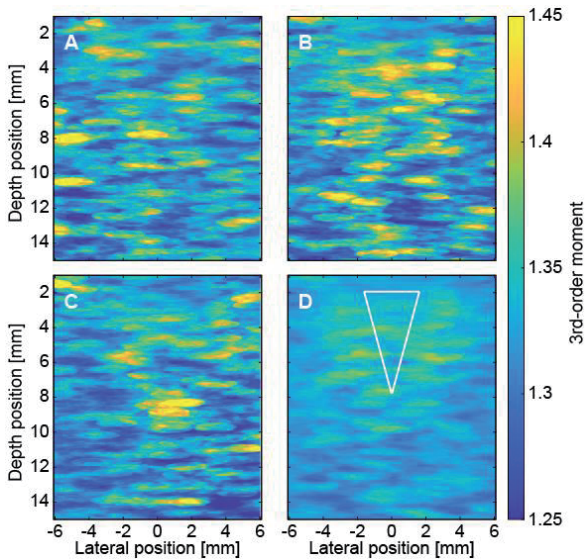Fig. 2 3rd-order-moment maps of ultrasound images acquired using L39-21gD, the steering angles of -15° (A), 0° (B), 15° (C), and the compounded one (D).
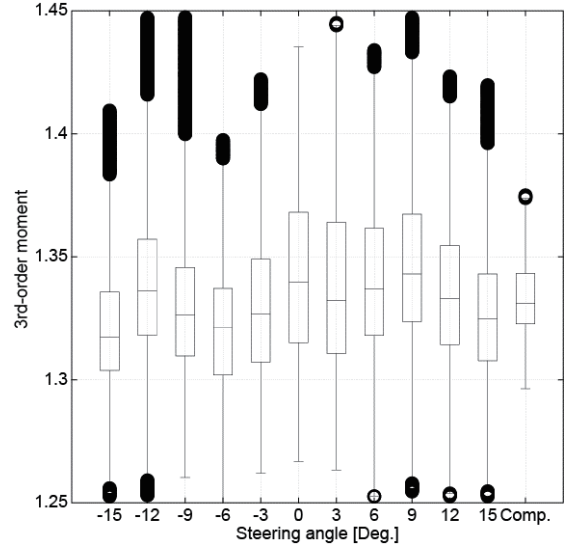

Fig. 3 Box-and-whisker plot of 3rd-order moments of ultrasound images acquired using L11-5v.

Fig. 4 Box-and-whisker plot of 3rd-order moments of ultrasound images acquired using L39-21gD.

1 was 3 times the depth and lateral of that in Fig. 2. In Figs. 3 and 4, the interquartile ranges of the 3rd-order moments are reduced by the compound. Therefore, it is suggested that the fluctuations in echo-envelope statistics can be suppressed by the compound.

4. Conclusion

In the echo-envelope analysis of ultrasound images, multiple different ultrasound images of the same region were formed by steering the ultrasound beam. Then, their 3rd-order moments were calculated and compounded to one 3rd-order-moment map. The statistical fluctuations of 3rd-order moments were suppressed by the compound. The improvement of stability of the echo-envelope statistics can be expected by the proposed method.
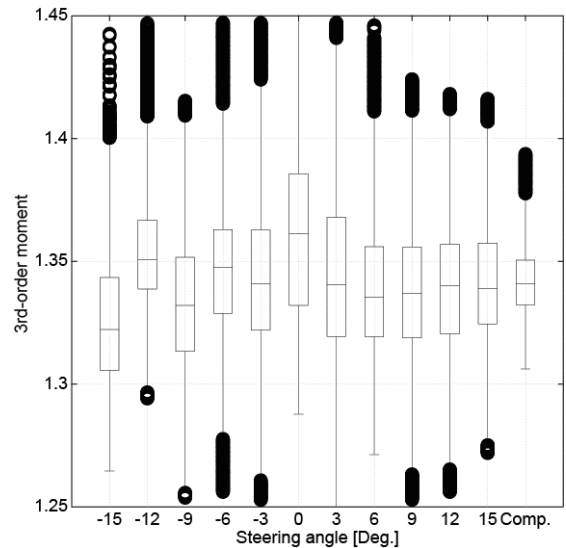
Acknowledgment

References

1) S. Mori, M. Arakawa, H. Kanai, and H. Hachiya, Jpn. J. Appl. Phys. **62** (SJ), SJ1045 (2023).